

Design and Simulation of Paddle Wheel Aerator with Movable Blades

Samsul Bahri

Department of Mechanical Engineering
Lhokseumawe State Polytechnic, Indonesia

Radite P.A. Setiawan

Department of Mechanical and Biosystem Engineering
Bogor Agricultural University, Indonesia

Wawan Hermawan

Department of Mechanical and Biosystem Engineering
Bogor Agricultural University, Indonesia

Muhammad Zairin Junior

Department of Aquaculture
Bogor Agricultural University, Indonesia

Abstract— The development of movable blade is based on fact that power is required only when blade of paddle wheel aerator entering water and in contrary action of aeration effect only when the blade is about leaving the water. This study was carried out to design and simulate paddle wheel aerator with movable blade which will open when entering water and close when leaving water. Wheel closed at quadrant I to IV (entering water surface) and was about to open at quadrant III to II (leaving water surface). The blade was designed referring to commonly used Taiwan wheel type. The component of movable blade mechanism consisted of cam and shaft, velg, velg cap, blade holder, follower, spring and bearing. Follower was able to rotate with angle of rotation was 125° , rotational displacement was 50 mm, maximum velocity was 0.55 m/s and acceleration was 6.09 m/s^2 . Average drag force using movable blade at operating depth 4 cm, 6 cm and 8 cm was 34.44 Nm, 55.54 Nm, and 93.37 Nm, respectively. Torque was 9.90 Nm, 15.54 Nm, and 23.41 Nm, respectively. The reduction torque was 26.90%, 35.96% and 23.74%, respectively. The largest angle of pressure occurred between cam and follower was 40.12° and the maximum torque required to rotate movable wheel was 80.09 Nm.

Keyword; Paddle wheel aerator; movable blade aerator; follower mechanism; drag force of aerator; torque of aerator

I. INTRODUCTION

Aerator is used to increase air and water contact by means of mechanical device. Paddle wheel aerator is one type of widely used aerator device in pond farming. Laksitanonta (2003) confirmed that paddle wheel aerator is considered as the most appropriate aerator device due to aeration mechanism and wide usable driven power.

Several parameters including water and air surface contact, differential oxygen concentration, film surface coefficient and turbulence influence aeration rate (Boyd 1998). Aeration performance was influenced by geometry, size and wheel velocity (Moulicket *al.* 2002). Higher size tends to have higher aeration which simultaneously followed by higher driven power needs due to higher drag force. This condition creates certain problem in utilizing paddle wheel aerator as it may increase operational cost including electrical and fuel consumption.

Aerator Taiwan model had standard aeration efficiency (SAE) value of $1.063 \text{ kg O}_2 \text{ kW h}^{-1}$ (Peterson & Walker 2002). Aerator designed by Bhuyaret *al.* (2009) had SAE value $2.269 \text{ kg O}_2 \text{ kWh}^{-1}$. The most appropriate paddle wheel aerator was designed by Moore and Boyd with SAE value $2.54 \text{ kg O}_2 \text{ kW h}^{-1}$. Some of fabrications use aerator design with specification of 2.25-7.5 kW and *SOTR* 17.4- 23.2 $\text{kg O}_2 \text{ h}^{-1}$ and average value of SAE was $2.2 \text{ kg O}_2 \text{ kW h}^{-1}$ (Moore & Boyd 1992).

Until now, the development of paddle wheel aerator still uses non-movable blade which result in less optimum power consumption because power is linear with the increasing of aeration rate. Therefore, development of movable blade is needed due to aeration power is only required when blade entering water and in contrary the aeration effect only occurs when blade is about to leaving the water. Therefore movable blade was designed to open when leaving water and close when entering water. This study was aimed to design and simulate paddle wheel aerator with movable blade to reduce drag force acting on blade as well as power consumption.

II. DESIGN METHOD

A. Design

Wheel was designed to rotate clockwise with movable blade that enabled to open and close. The blade was about to close at quadrant I to IV (entering water surface) and open at quadrant III to II (leaving water surface). Blade opened to 45° from its close position which parallel to rim. Wheel dimension was designed similarly with commonly used wheel size i.e. 20 cm width, 30 cm rim diameter and 60 cm total dimension.

B. Simulation

Simulation was carried out at different operating depths (*h*) and different follower position with a combination of rotational speed (*n*) of 115 rpm. Operating depth was set at 4, 6 and 8 cm at position 1 (follower was perpendicular to the water surface), position 2 (follower was rotated to 15°) and position 3 (follower was rotated to 30°).

Simulation was carried out using computational fluid dynamic. The type of analysis was external flow with x-axis as reference axis. The size of computational domain was $80 \times 30 \times 14 \text{ cm}$ and meshing was set at 2 mm (Figure 1). Fluid used in this experiment was water with temperature 25°C and

pressure 1 atm, density 997 kg/m^3 and dynamic viscosity $0.00089 \text{ Pa}^2 \text{ s}$.

Simulation was performed by setting fluid flow opposite to the statorwheel with tangential velocity was 3.372 m/s . The main results of the analysis were force, torque and contour.

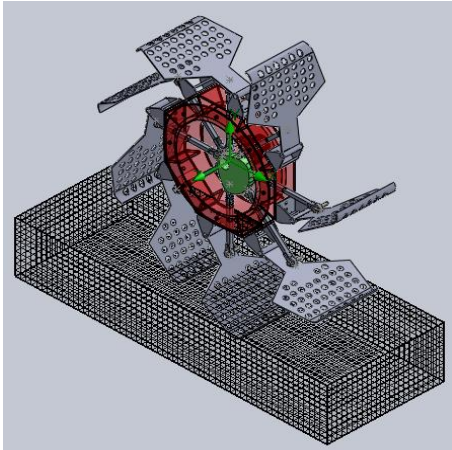


Fig. 1. Meshing domain

III. RESULT AND DISCUSSION

A. Structural Design

The wheel structure consisted of two main components i.e. stationary and rotary component as shown in Figure 2.

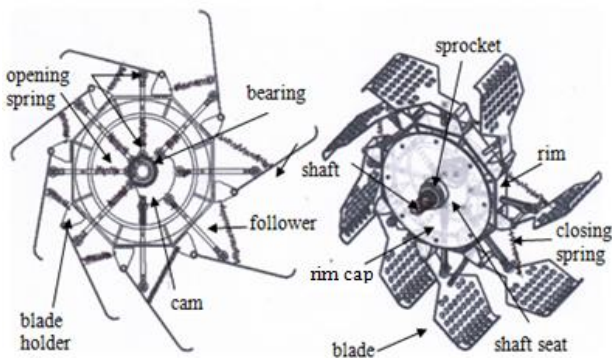


Fig. 2. Wheel structure with movable blade

Stationary component consisted of cam and shaft. The longest and shortest radius of cam were 680 mm and 17.5 mm , respectively. Cam was mounted to shaft with diameter of 25 mm and attached to machine frame.

Rotary component consisted of the rim, rim cap, blade holder, follower, bearing and spring. The rim was octagonal-shape encircling tube with diameter of 218 mm and height of 30 mm . One side of the tube was enclosed with metal sheet, shaft seat and bearing with diameter of 25 mm . Outside the shaft seat, sprocket that engage onto chain was attached for transmission purpose. The rim cap was a shaft seat made from metal sheet and similar bearing with rim tube which mounted to rim tube using bolt. Blade was used to directly bursting up water. Blades formed 30° of angle towards rim with radius of curvature was 40 cm . The size of the blade was 15 cm of

width, 20 cm of length, trapezoid-shape with 15° of bottom side and 30° of top side, had 40 holes with diameter of 1.6 cm . Blade holder was used to place blade with shaft of 8 mm and height of 25 mm and bolted at the end side of rim. The follower stem was used to push blade to open and close adjusting to cam profile. The follower stem was 150 mm of height and bearing with 19 mm of external diameter was attached on the two end-sides. Spring consisted of opening blade and closing blade. The opening spring was inserted to follower stem with diameter of the spring was 10.5 mm , length was 60 mm , wire diameter was 1 mm and spring constant was 0.35 Nm . The closing spring of blade was attached on the front blade holder with diameter of 10 mm , length of 45 mm , wire diameter of 1 mm and spring constant of 0.5 Nm .

B. Motion Mechanism

Movable blade were driven using cam mechanism. The cam is a simply mechanism that can provide almost all types of follower movement. The movement analysis of cam mechanism is shown in Figure 3.

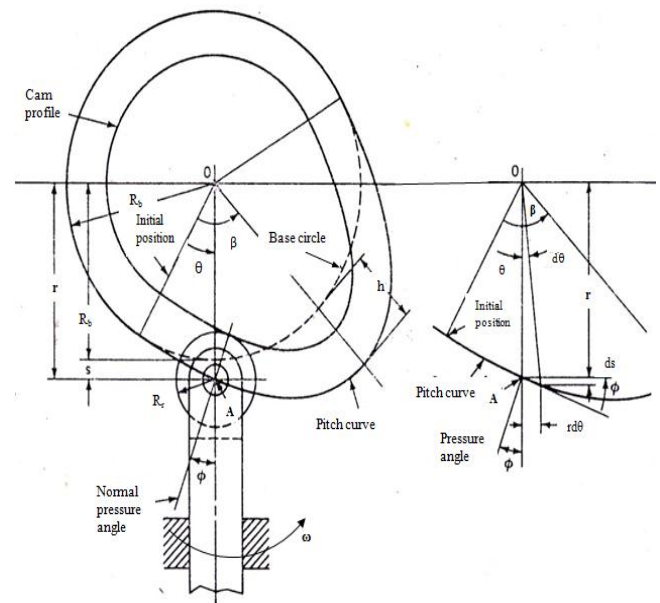


Fig. 3. Profile analysis of cam-follower

Diagram of displacement, velocity and acceleration of cam is important factors in determining cam design (Martin 1982). Equation of cam displacement is written as follows:

$$\begin{aligned} \text{for } \frac{\theta}{\beta} \leq 0.5 \quad s &= 2h \frac{\theta^2}{\beta^2} \\ \text{for } \frac{\theta}{\beta} \geq 0.5 \quad s &= h \left[1 - 2 \left(1 - \frac{\theta}{\beta} \right)^2 \right] \end{aligned} \quad (1)$$

Equation of cam velocity is written as follows:

$$\begin{aligned} \text{for } \frac{\theta}{\beta} \leq 0.5 \quad \frac{ds}{dt} &= \frac{4h\omega\theta}{\beta^2} \\ \text{for } \frac{\theta}{\beta} \geq 0.5 \quad \frac{ds}{dt} &= \frac{4h\omega}{\beta} \left(1 - \frac{\theta}{\beta} \right) \end{aligned} \quad (2)$$

Equation of cam acceleration is written as follows:

$$\text{for } \frac{\theta}{\beta} \leq 0.5 \quad \frac{d^2s}{dt^2} = \frac{4h\omega^2}{\beta^2}$$

for $\frac{\theta}{\beta} \geq 0.5$ $\frac{d^2s}{dt^2} = -\frac{4h\omega^2}{\beta^2}$ (3)

The result of follower displacement, velocity and acceleration is shown in Table 1.

TABLE I. MOTION OF FOLLOWER

θ (deg)	$2\pi\theta/\beta$ (deg)	t (s)	s (mm)	ds/dt (m/s)	d ² s/dt ² (m ² /s ²)
0	0	0.00	0	0.00	6.09
12.5	36	0.05	1	0.11	6.09
25	72	0.10	4	0.22	6.09
37.5	108	0.16	9	0.33	6.09
50	144	0.21	16	0.44	6.09
62.5	180	0.26	25	0.55	6.09
62.5	180	0.26	25	0.55	-6.09
75	216	0.31	34	0.44	-6.09
87.5	252	0.37	41	0.33	-6.09
100	288	0.42	46	0.22	-6.09
112.5	324	0.47	49	0.11	-6.09
125	360	0.52	50	0.00	-6.09

The maximum displacement of follower for one rotation 50 mm with angle of rotation 125° is shown in Figure 4.

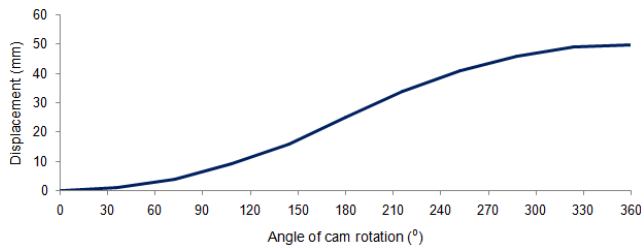


Fig. 4. Displacement of follower

The maximum velocity of follower was 0.55 m/s as shown in Figure 5.

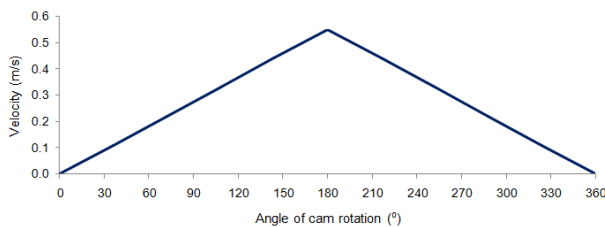


Fig. 5. Velocity of follower

The constant acceleration was 6.09 m/s² as shown in Figure 6.

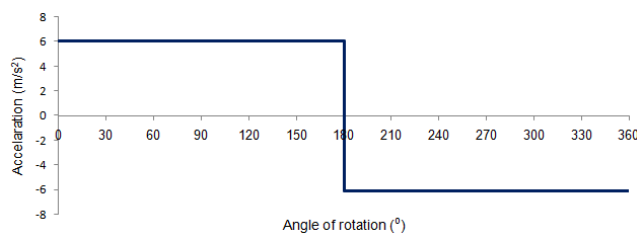


Fig. 6. Acceleration of follower

C. Angle of Pressure

Angle of pressure determines the smoothness of cam movement. The analysis of angle of pressure was illustrated in Figure 3. Angle of pressure (ϕ) for every angular position was equated as follows:

$r = R_b + s$

$\tan \phi = \frac{ds}{r d\theta}$ (4)

The magnitude of pressure angle for every angle of rotation is shown in Table 2.

TABLE II. PRESSURE ANGLE OF FOLLOWER

θ (deg)	$r=R_b+s$	$\tan\theta=ds/r(d\theta)$	ds/d θ	ϕ (deg)
0	27	0.00	0.00	0.00
36	28	9.17	0.33	18.13
72	31	18.33	0.59	30.60
108	36	27.50	0.76	37.38
144	43	36.67	0.85	40.46
180	52	45.84	0.88	41.40
180	52	45.84	0.88	41.40
216	61	36.67	0.60	31.01
252	68	27.50	0.40	22.02
288	73	18.33	0.25	14.10
324	76	9.17	0.12	6.88
360	77	0.00	0.00	0.00

The largest angle of pressure between cam and follower was 41.40°. This magnitude was too large and not necessary for cam-follower mechanism as it required high force and caused mechanism failure that led to machine damage.

D. Drag Force

Drag force of a blade is a drag that inhibit blade movement in a water. The most common drag force is friction force that parallel to object's surface and pressure force that perpendicular to object's surface. Drag force is applied as an dynamic fluid for an object that flow through fluid.

Drag force received by blade without using movable blade mechanism at operating depth of 4 cm, 6 cm and 8 cm for position 1, 2 and 3 was 51.35 N, 86.22 N, and 109.27, 47.48 N, 71.08 N and 110.51 N, and 54.67 N, 71.98 N and 106.70 N, respectively. While using movable blade mechanism at operating depth of 4 cm, 6 cm and 8 cm was 34.41 N, 55.52 N, and 93.69 N, 13.24 N, 43.10 N, and 60.63 N and 19.13 N, 37.28 N and 69.98 N, respectively (Figure 7).

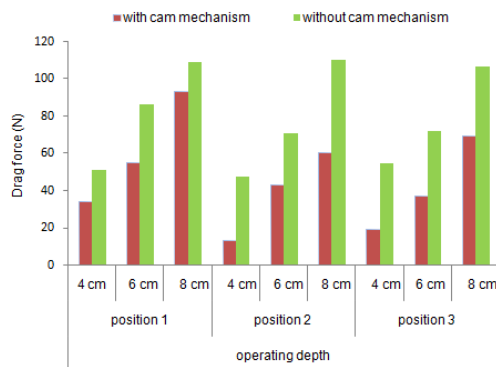


Fig. 7. Drag force of paddle wheel blade

contact surface area between blade and water as stated by Munson *et al* (2006).

Torque is a quantitative measure of a force to rotate or change the motion of an object. Torque that required by aerator is determined by the force acting and the perpendicular distance where the force is acted. Correlation between the magnitude of torque and the magnitude of power (P) of the aerator to rotate paddle wheel aerator at certain angular velocity (ω) was calculated as follows:

$$P = \tau \omega \tag{6}$$

Torque required by wheel without using movable blade mechanism at operating depth of 4 cm, 6 cm and 8 cm for position 1, 2 and 3 was 13.33 Nm, 23.89 Nm, and 31.28 Nm, 12.78 Nm, 20.19 Nm and 31.97 Nm, and 13.97 Nm, 18.88 Nm and 28.27 Nm, respectively. While torque required using movable blade mechanism at operating depth of 4 cm, 6 cm, dan 8 cm for position 1, 2 and 3 was 9.89 Nm, 15.54 Nm, and 23.45 Nm, 4.34 Nm, 12.33 Nm and 17.25 Nm, and 4.95 Nm, 9.19 Nm dan 17.65 Nm, respectively (Figure 8).

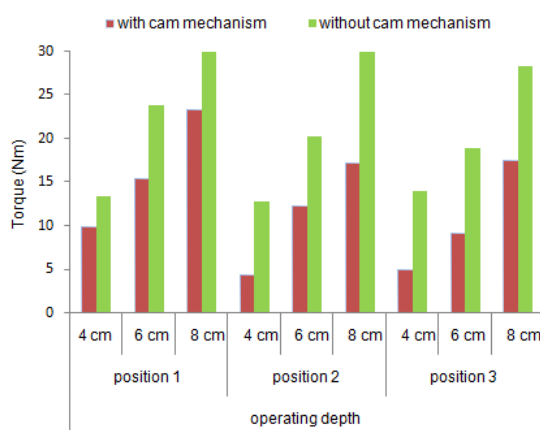


Fig. 8. Torque of wheel blade

Application of cam mechanism could reduce drag force of the wheel. The average reduction at operating depth of 4, 6 and 8 cm was 56.50%, 40.73% and 31.30%, respectively. While the average torque reduction using movable blade mechanism was 52.15%, 41.14% and 36.25%, respectively (Figure 9).

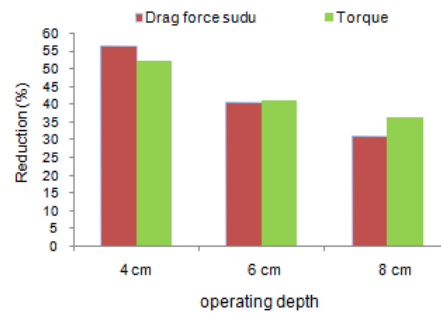


Fig. 9. Reduction of drag force and torque

According to the required torque, using Equation 6 and without calculating other mechanical loss, required power to rotate wheel using movable blade was about 0.34 kW. This magnitude of power was lower than commonly used standard power of fabricated-paddle wheel aerator which ranges between 2.25-7.7 kW (Moore & Boyd 1992).

E. Spring Mechanism

Each blade had two types of spring i.e. blade-closing spring and blade-opening spring. Blade-closing spring (s_1) worked against drag force (F_d) and gravity of the blade (w), while blade-opening spring (s_2) worked against force of blade-closing spring from cam pressure due to wheel rotation. Analysis of spring force is shown in Figure 10.

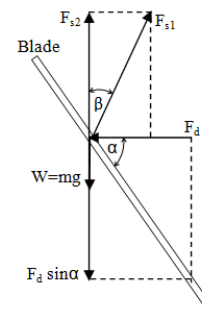


Fig. 10. Spring force analysis

Based on the calculation, some of spring data were collected, including installed length, operating length, operating force, springs material, wire diameter, average diameter, inside diameter, outside diameter, free length, number of coils and allowable shear stress for blade-opening springs. The magnitude was 75 mm, 25 mm, 2.45 N, 49.05 N, chromium-vanadium A231, 2 mm, 2 mm, 10.5 mm, 14.5 mm, 80 mm, 12 coils and 922.74 MPa, respectively. The magnitude for blade-closing spring was 124 mm, 38 mm, 2.45 N, 264.50 N, chromium-vanadium A231, 2 mm, 2 mm, 8 mm, 125 mm, 130 mm, 20 coils and 815.75 MPa, respectively.

F. Inertia and Torque

Inertia and torque analysis are shown in Figure 11. The influencing parameters consisted of force acting on follower (P), inertia force of follower (f), force of gravity on follower (W), shear stress acting on follower (F), normal force on rim towards follower (F_1, F_2), normal force of cam toward follower (N), follower overhang (a), distance between bearing surface (b), diameter of follower stem (d), pressure

angle (ϕ) and friction coefficient between follower (μ).

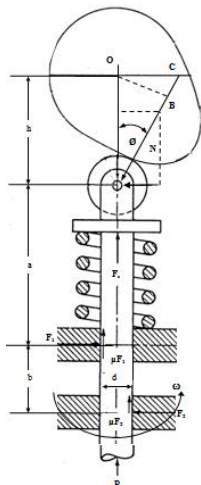


Fig. 11. Analysis of angle of pressure

Total force along follower axis was:

$$F = P + f + W + F_s$$

$$(5)$$

Total vertical force was:

$$N \cos \phi = F + \mu (F_1 + F_2) \tag{6}$$

Total horizontal force was:

$$F_1 = F_2 + N \sin \phi \tag{7}$$

Summing moments to a point where F_1 works, gave:

$$F_2 (b - \mu d) = N_a \sin \phi + \frac{d}{2} (F - N \cos \phi) \tag{8}$$

By neglecting F_1 and F_2 at the last 3 equations, normal force of cam acting on follower was:

$$N = \frac{F_b}{b \cos \phi - (2\mu a + \mu b - \mu^2 d) \sin \phi} \tag{9}$$

Torque required to rotate paddle wheel was calculated as follow:

$$T = N (OB) \tag{10}$$

The results of normal force, vertical force and horizontal force are shown in Table 3. The maximum torque required to activate blade mechanism was 80.09 Nm.

Based on the required torque, using equation 6 and neglecting other mechanical loss, as much as 0.96 kW was required to rotate movable blade on paddle wheel aerator.

TABLE III. NORMAL FORCE OF CAM-FOLLOWER

θ (deg)	$2\pi\theta/\beta$ (deg)	ϕ (deg)	N (N)	Nx (N)	Ny (N)
0	0	0	239.64	239.64	0
12.5	36	18.13	-380.96	-362.05	-118.54
25	72	30.60	-146.87	-126.41	-74.77
37.5	108	37.38	-120.09	-95.43	-72.91
50	144	40.46	-122.97	-93.57	-79.79
62.5	180	41.40	-144.87	-108.68	-95.80
62.5	180	41.40	-144.87	-108.68	-95.80
75	216	31.01	-324.70	-278.29	-167.29
87.5	252	22.02	-3141.54	-2912.37	-1177.88
100	288	14.10	612.74	594.28	149.26
112.5	324	6.88	328.35	325.99	39.32
125	360	0	239.64	239.64	0

G. Fluid Velocity

Fluid velocity contour occurred at wheel without using movable blade is shown in Figure 12.

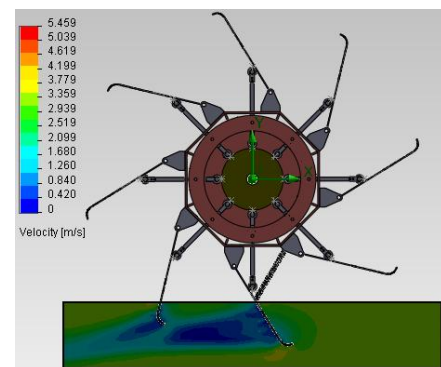


Fig. 12. Fluid velocity contour of fluid without using movable blade mechanism

Fluid velocity contour occurred at wheel using movable blade mechanism is shown in Figure 13.

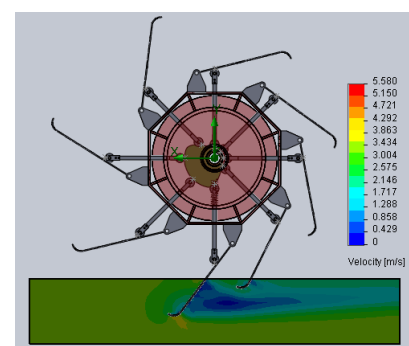


Fig. 13. Fluid velocity contour using movable blade

Blade pushing flow pattern showed slight similar flow pattern. Blade outcoming flow pattern showed that wheel using movable blade mechanism had better flow pattern which indicated by more uniform velocity.

IV. CONCLUSION

The wheel structure consisted of two main components i.e. stationary and rotary component. Stationary component consisted of cam and shaft. Rotary component consisted of a rim, a rim cap, blade holders, followers, bearings and springs. The follower was able to rotate with angle of rotation was 125° , rotational displacement was 50 mm, maximum velocity was 0.55 m/s and acceleration was 6.09 m/s^2 . The follower had constant acceleration. Average torque which required by the paddle wheel using movable blade at operating depth of 4 cm, 6 cm and 8 cm were 9.90 Nm, 15.54 Nm, and 23.41 Nm, respectively. The drag force were 34.44 Nm, 55.54 Nm, and 93.37 Nm, respectively. Torque reduction due to the used of movable blade at operating depth of 4 cm, 6 cm, and 8 cm were 26.90%, 35.96% and 23.74%, respectively. The largest angle of pressure occurred between cam and follower was 40.12° . The maximum torque required to rotate movable blade was 80.09 Nm. Machine torque was largely used to activate movable blade mechanism rather than to use for reducing drag force.

REFERENCES

- [1] Laksitanonta S, Singh S, and Singh G, A review of aerators and aeration practices in Thai Aquaculture, "Agricultural Mechanization in Asia, Africa and Latin America 34 (4):64-71. 2003.
- [2] Moore JM and Boyd CE, "Design of small paddle wheel aerators," *Aquac Eng* 11:55-69. 1992.
- [3] Moulick S, Mal BC, and Bandyopadhyay, "Prediction of aeration performance of paddlewheel aerators," *AquacEng* 25:217-237.2002.
- [4] Peterson EL and Walker MB, "Effect of speed on Taiwanese paddelwheel aeration," *AquacEng* 26:129-147. 2002.
- [5] Wyban JA, Pruder GD, and Leber KM, "Paddle wheel effect on shrimp growth, production and crop value in commercial earthen ponds," *J World Aquac Soc* 20:18-23. 1989.
- [6] Bhuyar LB, Thakre SB, and Ingole NW, "Design characteristics of curved blade aerator w.r.t. aeration efficiency and overall oxygen transfer coefficient and comparison with CFD modeling," *International Journal of Engineering, Science and Technology* 1: 1-15.2009.
- [7] Boyd CE, "Pond water aeration systems," *AquacEng* 18:9-40.1998.
- [8] Martin, GH, "Kinematics and dynamics of machines" USA: McGraw-Hill, Ltd. 194-382, 1982.
- [9] Munson, Young, and Okiishi, "Fundamentals of fluid mechanics" USA : John Wiley & Sons, Inc. 518-538, 2006.